

Electronic Supplementary Information

Side Chain Engineering of Polymer Acceptors for All-Polymer Solar Cells with Enhanced Efficiency

Huiliang Sun,^a Bin Liu,^{a,b} Zaiyu Wang,^c Shaohua Ling,^a Yujie Zhang,^a Guangye Zhang,^d Yang Wang,^a Ming Zhang,^c Bolin Li,^a Wanli Yang,^a Junwei Wang,^a Han Guo,^a Feng Liu*^c and Xugang Guo*^a

^a Department of Materials Science and Engineering and The Shenzhen Key Laboratory for Printed Organic Electronics, Southern University of Science and Technology (SUSTech), No. 1088, Xueyuan Road, Shenzhen, Guangdong, 518055, China
E-Mail: guoxg@sustech.edu.cn

^b School of Chemistry and Chemical Engineering, Shanghai Jiaotong University, 800 Dongchuan Road, Shanghai 200240, China
E-mail: fengliu82@sjtu.edu.cn

^c eFlexPV Limited (China), Room 228, Block 11, Jin Xiu Da Di, No. 121 Hu Di Pai, Song Yuan Sha Community, Guanhu Street, Longhua District, Shenzhen, China.

^d School of Advanced Materials, Peking University Shenzhen Graduate School, Peking University, Shenzhen 518055, China

Keywords: fused bithiophene imide oligomers, side chain engineering, all-polymer solar cells, polymer acceptors, morphology

1. Materials and Instruments

All reagents and chemicals were commercially available and were used without further purification unless otherwise stated. Anhydrous toluene was distilled from Na/benzophenone under argon. 3,4-difluoro-2,5-bis(trimethylstannyl)thiophene was purchased from Derthon Optoelectronic Materials Science Technology Co., Ltd. (Shenzhen, Guangdong, China). Unless otherwise stated, all reactions were carried out under inert atmosphere using standard Schlenk-line techniques. The known compound BTI2 monomers (BTI2-OD and BTI2-DT) with different alkyl side chain were synthesized following the prior work.^{1, 2} NMR spectra were recorded on Bruker Ascend 400 MHz spectrometer. Elemental analyses of compounds were performed at Changchun Institute of Applied Chemistry Chinese Academy of Sciences (Changchun, Jilin). High-resolution mass spectrometry was obtained on Thermo Scientific™ Q-Exactive. Molecular weight of the polymers was measured using a high-temperature gel permeation chromatography (GPC, Agilent PL-GPC220) at 150 °C with 1,2,4-trichlorobenzene as the eluent and polystyrenes as the standards. UV/vis absorption spectra of polymer solution and films were recorded on a Shimadzu UV-3600 UV/Vis-NIR spectrophotometer. Cyclic voltammetry measurements of all polymer films were carried out under argon atmosphere using a CHI760 Voltammetry Workstation with N₂-saturated solution of 0.1 M tetra(*n*-butyl) ammonium hexafluorophosphate (Bu₄NPF₆) in acetonitrile (CH₃CN) as the supporting electrolyte. A platinum disk working electrode, a platinum wire counter electrode, and a silver wire reference electrode were employed, and the ferrocene/ferrocenium (Fc/Fc⁺) redox couple was used as the reference for all measurements with a scanning rate of 50 mV s⁻¹. Thermogravimetric (TGA) measurements were carried out with a METTLER TOLEDO (TGA 1 STAR^e System) apparatus at a heating rate of 10 °C min⁻¹ under N₂. Differential scanning calorimetry (DSC) curves were recorded on Mettler, STAR^e with a heating ramp of 10 °C min⁻¹ in nitrogen. Steady-state photoluminescence (PL) spectra were measured using a Horiba iHR320 spectrometer with the Andor Newton EMCCD detector. PL spectra were excited using

a Coherent 532 CW laser. Atomic force microscopy (AFM) measurements of all-polymer blend films were conducted using a Dimension Icon Scanning Probe Microscope (Asylum Research, MFP-3D-Stand Alone) in the tapping mode. Transmission electron microscopy (TEM) specimens were prepared following the identical conditions as the actual devices, but were drop-cast onto a 40 nm PEDOT:PSS covered substrate. After drying, the substrates were transferred to deionized water and the floated films were transferred onto TEM grids. TEM images were obtained on Tecnai Spirit (20 kV) TEM. Two-dimensional grazing incident wide angle X-ray scattering (2D-GIWAXS) measurements were carried out at the PLS-II 9A U-SAXS beam line of Pohang Accelerator Laboratory, Korea. The external quantum efficiency (EQE) was recorded by a QE-R3011 measurement system (Enli Technology, Inc.).

Polymerization of PBTI2(0DT)-FT²: To a 5 mL reaction tube equipped with a stirring bar, the distannylated monomer 3,4-difluoro-2,5-bis(trimethylstannyl)thiophene (0.1 mmol), BTI2-OD (0.1 mmol), Pd₂(dba)₃ (1.37 mg, 0.0015 mmol), P(*o*-tolyl)₃ (3.65 mg, 0.012 mmol), and toluene (2.5 mL) were added. The tube was purged with argon and sealed. The reaction tube was then set into a microwave reactor and heated to 140 °C for 3 h. Finally, 0.2 mL 2-bromothiophene was added and the reaction mixture was stirred at 140 °C for another 0.5 h, then 2-(tributylstannyl)thiophene was added and stirred at 140 °C for another 0.5 h. After cooling to room temperature, the reaction solution was dripped into 80 mL methanol containing HCl under vigorous stirring and stirred for 1 h. Then the precipitated solid was filtered by a thimble and subjected to the sequential Soxhlet extraction with methanol, hexane and dichloromethane as the solvents to remove impurities and low molecular weight fractions. The residue was extracted with chloroform as the final solvent and the chloroform solution was concentrated to ~ 20 mL and precipitated into 100 mL methanol. The precipitate was dried in vacuo to yield the product polymer as a dark blue solid. Anal. Calcd. For BTI2-ODT: C, 66.51; H, 7.56; N, 2.50. Found: C, 66.03; H, 7.63; N, 2.45. ¹H NMR (400 MHz, C₂D₂Cl₄, 120 °C) δ: 4.44 (m, 4H), 2.39-0.96 (m, 78H).

Polymerization of PBTI2(30DT)-FT: To a 5 mL reaction tube equipped with a stirring bar, distannylated monomer 3,4-difluoro-2,5-bis(trimethylstannyl)thiophene (0.1 mmol) and BTI2-BTI2-OD (81.08 mg, 0.07 mmol) and BTI2-DT (38.11 mg, 0.03 mmol), Pd₂(dba)₃ (1.37 mg, 0.0015 mmol), P(*o*-tolyl)₃ (3.65 mg, 0.012 mmol), and toluene (2.5 mL) were added. The tube was purged with argon and sealed. The next steps were the same as those followed for the polymerizations of PBTI2(0DT)-FT. The polymerization yields and GPC results are shown in Table 1. Anal. Calcd. For BTI2-30DT: C, 67.03; H, 7.75; N, 2.43. Found: C, 67.12; H, 7.83; N, 2.41. ¹H NMR (400 MHz, C₂D₂Cl₄, 120 °C) δ: 4.46 (m, 8H), 2.39-0.97 (m, 165H).

Polymerization of PBTI2(50DT)-FT: To a 5 mL reaction tube equipped with a stirring bar, distannylated monomer 3,4-difluoro-2,5-bis(trimethylstannyl)thiophene (0.1 mmol) and dibrominated monomer BTI2-OD (57.92 mg, 0.05 mmol) and BTI2-DT (63.52 mg, 0.05 mmol), Pd₂(dba)₃ (1.37 mg, 0.0015 mmol), P(*o*-tolyl)₃ (3.65 mg, 0.012 mmol), and toluene (2.5 mL) were added. The tube was purged with argon and sealed. The next steps were the same as those followed for the polymerizations of PBTI2(0DT)-FT. The GPC results are shown in Table S1. Anal. Calcd. For BTI2-50DT: C, 67.38; H, 7.87; N, 2.38. Found: C, 67.40; H, 7.89; N, 2.32. ¹H NMR (400 MHz, C₂D₂Cl₄, 120 °C) δ: 4.49 (m, 8H), 2.41-0.98 (m, 172H).

Polymerization of PBTI2(70DT)-FT: To a 5 mL reaction tube equipped with a stirring bar, distannylated monomer 3,4-difluoro-2,5-bis(trimethylstannyl)thiophene (0.1 mmol) and dibrominated monomer BTI2-OD (34.75 mg, 0.03 mmol) and BTI2-DT (88.93 mg, 0.07 mmol), Pd₂(dba)₃ (1.37 mg, 0.0015 mmol), P(*o*-tolyl)₃ (3.65 mg, 0.012 mmol), and toluene (2.5 mL) were added. The tube was purged with argon and sealed. The next steps were the same as those followed for the polymerizations of PBTI2(0DT)-FT. The GPC results are shown in Table S1. Anal. Calcd. For BTI2-70DT: C, 67.74; H, 7.99; N, 2.34. Found: C, 67.83; H, 8.02; N, 2.30. ¹H NMR (400 MHz, C₂D₂Cl₄, 120 °C) δ: 4.49 (m, 8H), 2.39-0.99 (m, 178H).

Polymerization of PBTI2(100DT)-FT: To a 5 mL reaction tube equipped with a stirring bar, distannylated monomer 3,4-difluoro-2,5-bis(trimethylstannyl)thiophene (0.1 mmol) and dibrominated monomer BTI2-DT (0.1 mmol), Pd₂(dba)₃ (1.37 mg, 0.0015 mmol), P(*o*-tolyl)₃ (3.65 mg, 0.012 mmol), and toluene (2.5 mL) were added. The tube was purged with argon and sealed. The next steps were the same as those followed for the polymerizations of PBTI2(0DT)-FT. The GPC results are shown in Table 1. Anal. Calcd. For BTI2-100DT: C, 68.25; H, 8.18; N, 2.27. Found: C, 68.32; H, 8.20; N, 2.23. ¹H NMR (400 MHz, C₂D₂Cl₄, 120 °C) δ: 4.46 (m, 8H), 2.44-1.01 (m, 188H).

Table S1. Basic properties of polymer acceptors.

Polymer	M_n^a	PDI	λ_{onset}	$E_g^{\text{opt } b}$	HOMO ^c	LUMO ^c
acceptor	(KDa)		in film (nm)	(eV)	(eV)	(eV)
PBTI2(0DT)-FT	23.0	2.2	675	1.84	-6.13	-3.39
PBTI2(30DT)-FT	20.2	2.6	675	1.84	-6.14	-3.44
PBTI2(50DT)-FT	23.6	2.7	675	1.84	-6.14	-3.43
PBTI2(70DT)-FT	18.6	2.4	675	1.84	-6.12	-3.47
PBTI2(100DT)-FT	19.0	2.5	675	1.84	-6.09	-3.48

^{a)} Determined by gel permeation chromatography (GPC); ^{b)} $E_g^{\text{opt}} = 1240/\lambda_{\text{onset}}$; ^{c)} Calculated from cyclic voltammetry.

2. Thermogravimetric Analyses (TGA) and Differential Scanning Calorimetry (DSC)

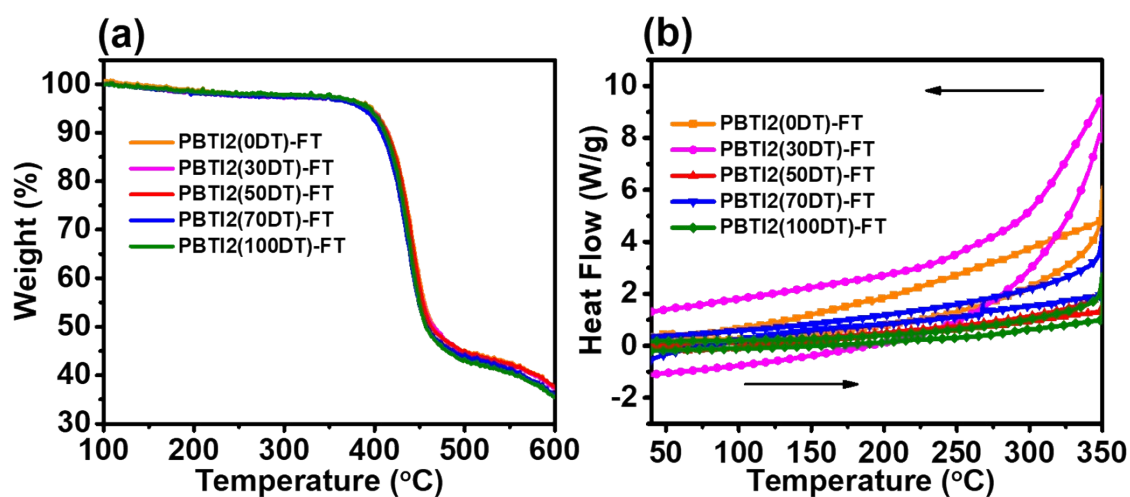


Figure S1. (a) Thermogravimetric analysis (heating ramp: 10 °C min⁻¹) of polymers. Nitrogen was used as the purge gas for TGA measurement; (b) DSC thermograms of polymers from the second heating and cooling scans (heating ramp: 10 °C min⁻¹)

3. UV/Vis absorption spectra

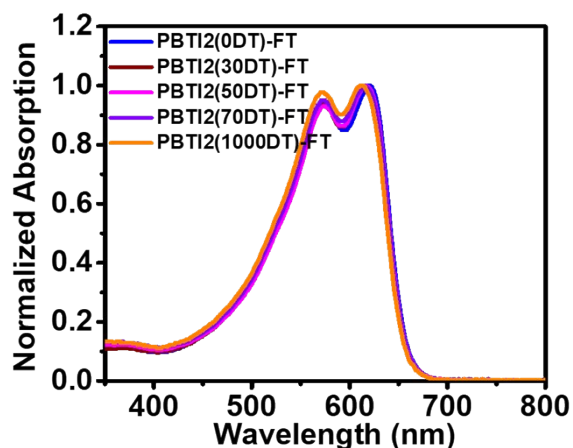


Figure S2. UV/Vis absorption spectra of polymers in CHCl_3 (10^{-5} mol/L)

4. SCLC Mobility Measurement.

Hole and electron mobilities were measured using the space-charge-limited current (SCLC) method.¹ The structure of ITO/PEDOT:PSS/active layer/ MoO_3 /Ag was used for hole-only devices and the structure of ITO/ ZnO /active layer/Ca/Al was used for electron-only devices, respectively. The SCLC mobilities were calculated by the MOTT-Gurney equation:

$$J = \frac{9}{8} \epsilon_0 \epsilon_r \mu \frac{V^2}{d^3}$$

Where J is the current density, ϵ_r is the relative dielectric constant of active layer material, usually 2- 4 for organic semiconductors, herein we use a relative dielectric constant of 3 for polymer. ϵ_0 is the permittivity of empty space, μ is the mobility of hole or electron and d is the active layer thickness, V is the internal voltage in the device, and $V = V_{\text{appl}} - V_{\text{bi}}$, where V_{appl} is the voltage applied to the device, and V_{bi} is the built-in voltage resulting from the relative work function difference between the two electrodes (in the hole-only and the electron-only devices, the V_{bi} values can be neglected).

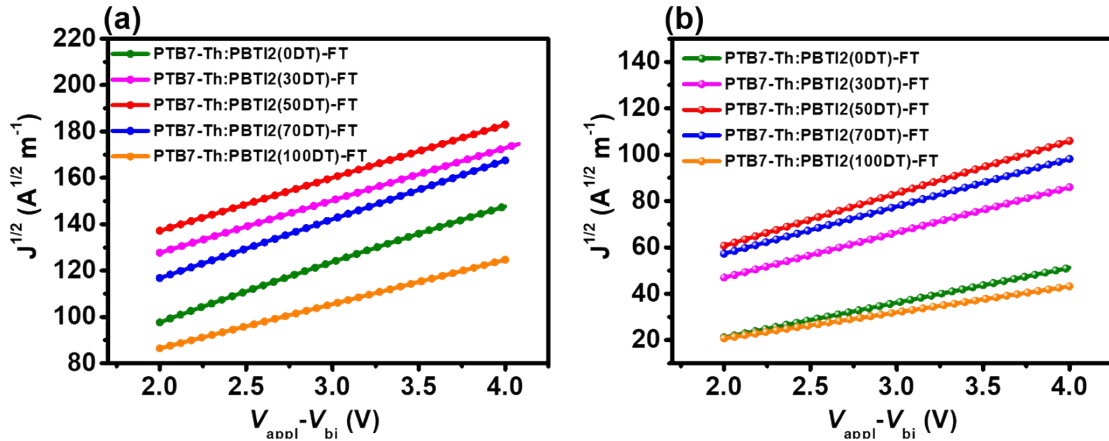


Figure S3. The corresponding $J^{1/2}$ - V curves for the hole-only (a) and electron-only (b) devices based on the blend films (in dark). For the electron-only device, the device structure is ITO/ZnO/ PTB7-Th:polymer acceptors/Ca/Al; while for hole-only device, the device structure is ITO/PEDOT:PSS/ PTB7-Th:polymer acceptors/MoO₃/Ag.

5. Photoluminescence Spectra.

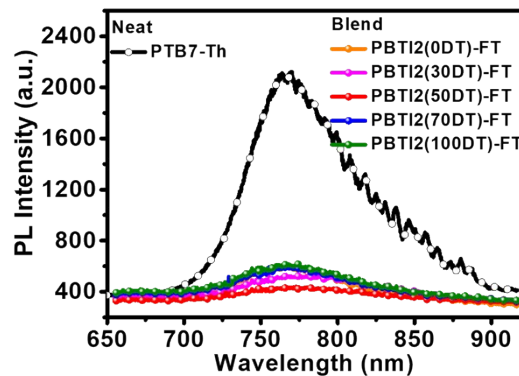


Figure S4. Photoluminescent (PL) spectra of PTB7-Th neat film and all blend films excited at 650 nm.

6. All-PSC Fabrication and Characterization.

Fabrication of Polymer Solar Cells with Conventional Structure: pre-patterned ITO-coated glass with a sheet resistance of $12 \Omega \text{ sq}^{-1}$ is used as the substrate, which is cleaned by sequential sonication in H₂O containing detergent, deionized H₂O, acetone, and isopropanol followed by drying in vacuum oven and then UV-ozone (BZS250GF-TC, HWOTECH, Shenzhen) treatment for 15 min. PEDOT:PSS (Clevios P VP A1 4083) was spin-coated onto the UV-ozone treated

ITO substrates, at 3000 rpm for 25 s then annealed at 150 °C for 15 min in air, forming ~40 nm film. The PEDOT:PSS-coated ITO substrates were transferred into a N₂-filled glove box for subsequent steps. The active layer solutions with various weight ratios were prepared at a total concentration of 18 mg mL⁻¹ in chlorobenzene (CB) without any additives. The solutions were stirred overnight to be completely dissolved. The active layer with an optimal thickness of ~115 nm is spin-coated onto PEDOT:PSS solutions. Then 0.8 nm LiF and 120 nm Al are sequentially deposited atop the active layer via thermal evaporation (*ca.* 1 × 10⁻⁵ Pa) to enable the effective area of 0.045 cm² for the solar cells. Before measuring the performance parameters of solar cells, all devices were thermally annealed at 80 °C for 5 min. For device characterization, all current-voltage (*J-V*) characteristics of the devices were measured under simulated AM1.5G irradiation (100 mW/cm²) using a Xe lamp-based SS-F5-3A Solar Simulator (Enli Technology, Inc.). A Xe lamp equipped with an AM1.5G filter was used as the white light source. The light intensity was controlled with an NREL-calibrated Si solar cell with a KG-5 filter. The external quantum efficiency (EQE) was measured by a QE-R3011 measurement system (Enli Technology, Inc.).

Table S2. Device performance parameters of conventional all-PSCs using various additive (DIO, ODT, CN or DPE) (1%, v/v) (Device structure: ITO/PEDOT:PSS/active layer/LiF/Al; D/A ratio = 1:2 (w/w); Concentration: 18mg mL⁻¹; Solvent: CB).

Active Layer	Additive	V_{oc} (V)	J_{sc} (mA cm ⁻²)	FF (%)	$PCE_{max/ave}$ (%)
PTB7- Th:PBTI2(30DT)-FT	DIO	1.02	12.29	50.20	6.27/6.13
	ODT	1.03	12.44	49.10	6.32/6.21
	CN	1.02	12.43	49.91	6.36/6.27
	DPE	1.03	12.67	49.33	6.43/6.36
PTB7-Th: PBTI2(50DT)-FT	DIO	1.03	13.55	51.74	7.20/7.04
	ODT	1.01	13.41	53.81	7.32/7.20
	CN	1.02	13.97	52.30	7.48/7.32
	DPE	1.01	13.68	54.69	7.54/7.38
PTB7-Th: PBTI2(70DT)-FT	DIO	1.03	9.79	52.36	5.26/5.11
	ODT	1.02	9.97	52.35	5.33/5.18
	CN	1.03	10.15	52.01	5.43/5.29

	DPE	1.01	11.53	47.25	5.51/5.36
	DIO	1.01	8.22	41.09	3.43/3.28
PTB7-Th:	ODT	1.03	8.39	41.22	3.55/3.42
PBTI2(100DT)-FT	CN	1.03	8.79	39.88	3.61/3.49
	DPE	1.04	8.46	41.83	3.66/3.53

Table S3. Device performance parameters of conventional all-PSCs with or without annealing (Device structure: ITO/PEDOT:PSS/active layer/LiF/Al; D/A ratio = 1:2 (w/w); Concentration: 18mg mL⁻¹; Post-annealing: 80°C for 5 min).

Active Layer	Annealing	V_{oc} (V)	J_{sc} (mA cm ⁻²)	FF (%)	PCE _{max/ave} (%)
PTB7-Th: PBTI2(30DT)-FT	Without annealing	1.02	12.21	51.89	6.43/6.27
	Post-annealing	1.01	12.78	53.06	6.85/6.54
PTB7-Th: PBTI2(50DT)-FT	Without annealing	1.01	13.61	57.33	7.90/7.72
	Post-annealing	1.01	13.96	59.03	8.32/8.09
PTB7-Th: PBTI2(70DT)-FT	Without annealing	1.03	10.96	51.94	5.84/5.71
	Post-annealing	1.03	11.51	52.65	6.23/5.87
PTB7-Th: PBTI2(100DT)-FT	Without annealing	1.02	8.53	46.49	4.05/3.84
	Post-annealing	1.02	8.95	47.05	4.30/3.99

Table S4. Device performance parameters of conventional all-PSCs with different electron transporting layers (ETLs). (Device structure: ITO/PEDOT:PSS/active layer/ETLs/Al; D/A ratio = 1:2 (w/w); Post-annealing: 80°C for 5 min).

Active Layer	ETL	V_{oc} (V)	J_{sc} (mA cm ⁻²)	FF (%)	PCE _{max/ave} (%)
PTB7-Th: PBTI2(30DT)-FT	PFN	1.02	12.25	50.31	6.30/6.19
	PFN-Br	1.02	12.70	50.12	6.47/6.32
	PDINO	1.03	12.61	50.62	6.55/6.42
	LiF	1.01	12.78	53.06	6.85/6.54
PTB7-Th: PBTI2(50DT)-FT	PFN	1.02	13.86	50.97	7.18/7.05
	PFN-Br	1.02	12.98	55.29	7.31/7.16
	PDINO	1.02	13.20	54.85	7.39/7.29
	LiF	1.01	13.96	59.03	8.32/8.09
PTB7-Th: PBTI2(70DT)-FT	PFN	1.02	10.70	50.15	5.49/5.36
	PFN-Br	1.03	10.61	52.03	5.66/5.47
	PDINO	1.02	10.78	53.16	5.85/5.71
	LiF	1.03	11.51	52.65	6.23/5.87

	PFN	1.03	8.24	41.21	3.51/3.37
PTB7-Th:	PFN-Br	1.03	8.38	42.26	3.65/3.52
PBTI2(100DT)-FT	PDINO	1.01	8.36	44.32	3.76/3.61
	LiF	1.02	8.95	47.05	4.30/3.99

Table S5. Summary of packing parameters of neat films

Polymer	Peak Location (\AA^{-1})(010)	π - π stack d-spacing (\AA)	Peak Location (\AA^{-1})(100)	lamellar-spacing d-spacing (\AA)
PBTI2(0DT)-FT	1.7722	3.5436181	0.23673	26.5281122
PBTI2(50DT)-FT	1.7683	3.55143358	0.23279	26.9771038
PBTI2(100DT)-FT	1.7677	3.55263902	0.22712	27.6505812

Table S6. Summary of crystal coherence length of neat films.

Polymer	FWHM(\AA^{-1})(010)	CCL(\AA)(010)	FWHM(\AA^{-1})(100)	CCL(\AA)(100)
PBTI2(0DT)-FT	0.11770	48.6	0.073959	77.4
PBTI2(50DT)-FT	0.11943	47.9	0.057631	99.3
PBTI2(100DT)-FT	0.11909	48.1	0.047935	119.4

Table S7. Summary of packing parameters of blend films

Blend	Peak Location (\AA^{-1})(010)	π - π stack d-spacing (\AA)	Peak Location (\AA^{-1})(100)	lamellar-spacing d-spacing (\AA)
PBTI2(0DT)-FT	1.7699	3.54822306	0.25405	24.7195434
PBTI2(50DT)-FT	1.7716	3.54481824	0.24224	25.9247028
PBTI2(100DT)-FT	1.7652	3.55767052	0.23578	26.6349987

Table S8. Summary of blend crystal coherence length.

Blend	FWHM(\AA^{-1})(010)	CCL(\AA)(010)	FWHM(\AA^{-1})(100)	CCL(\AA)(100)
PBTI2(0DT)-FT	0.12237	46.8	0.09115	62.8
PBTI2(50DT)-FT	0.12075	47.7	0.07606	75.3
PBTI2(100DT)-FT	0.12445	46.0	0.06663	85.9

Table S9. Hole and Electron Mobilities of all-PSCs Incorporating PTB7-Th:PA blend films.

Device ^a	μ_h (cm ² V ⁻¹ s ⁻¹) ^b	μ_e (cm ² V ⁻¹ s ⁻¹) ^b	$\mu_h\mu_e$
PTB7-Th:PBTI2(0DT)-FT	5.13×10^{-4}	1.82×10^{-5}	2.82
PTB7-Th:PBTI2(30DT)-FT	2.60×10^{-4}	1.93×10^{-4}	1.34
PTB7-Th:PBTI2(50DT)-FT	3.03×10^{-4}	2.96×10^{-4}	1.02
PTB7-Th:PBTI2(70DT)-FT	2.87×10^{-4}	1.86×10^{-4}	1.54
PTB7-Th:PBTI2(100DT)-FT	2.11×10^{-4}	7.09×10^{-5}	2.98

^aPTB7-Th:P_A = 1:2 (w/w); the device area is 4.5 mm². ^bAverage values with standard deviation were obtained from 5 devices.

Table S10. Device performance parameters for storage lifetime of the solar cells made from the PTB7-Th:PBTI2(50DT)-FT in a nitrogen-fill glovebox in the dark.

Store Time	V_{oc} (V)	J_{sc} (mA cm ⁻²)	FF (%)	PCE (%)
0	1.01	13.93	58.76	8.27
24	1.01	13.87	57.44	8.06
48	1.02	13.72	57.19	7.99
72	1.01	13.64	56.54	7.81
96	1.01	13.63	56.14	7.74
144	1.01	13.57	56.03	7.67
192	1.02	13.49	54.81	7.51
240	1.01	13.44	54.16	7.36
288	1.01	13.41	54.05	7.35
336	1.02	13.39	53.54	7.28
384	1.01	13.28	52.91	7.11

Table S11. Normalized PCE for storage lifetime of the solar cells made from the different type organic solar cells in a nitrogen-fill glovebox in the dark.

Store Time	PBTI2(50DT)-FT (%)	PBTI2(100DT)-FT (%)	N2200 (%)	ITIC (%)	PC ₇₁ BM (%)
0	100.00	100.00	100.00	100.00	100.00
24	97.49	96.89	98.29	95.16	93.57
48	96.68	94.53	96.55	90.20	85.13

72	94.47	92.79	94.80	81.27	75.03
96	93.62	91.79	91.46	70.80	68.55
144	92.74	89.35	89.63	61.83	61.11
192	90.85	88.38	87.55	54.94	52.92
240	89.03	86.20	86.10	51.82	47.71
288	88.93	85.11	83.71		
336	88.07	82.96	81.74		
384	86.05	81.63	81.06		

7. NMR of PBTI2(xDT)-FT

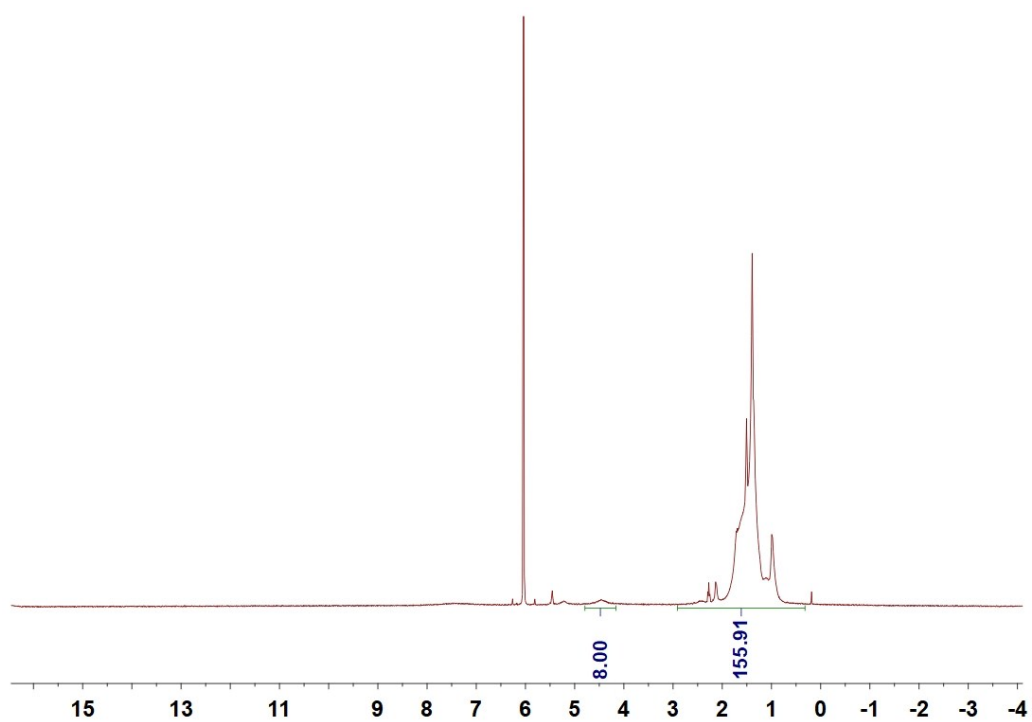


Figure S10. ¹H NMR spectrum of PBTI2(0DT)-FT.

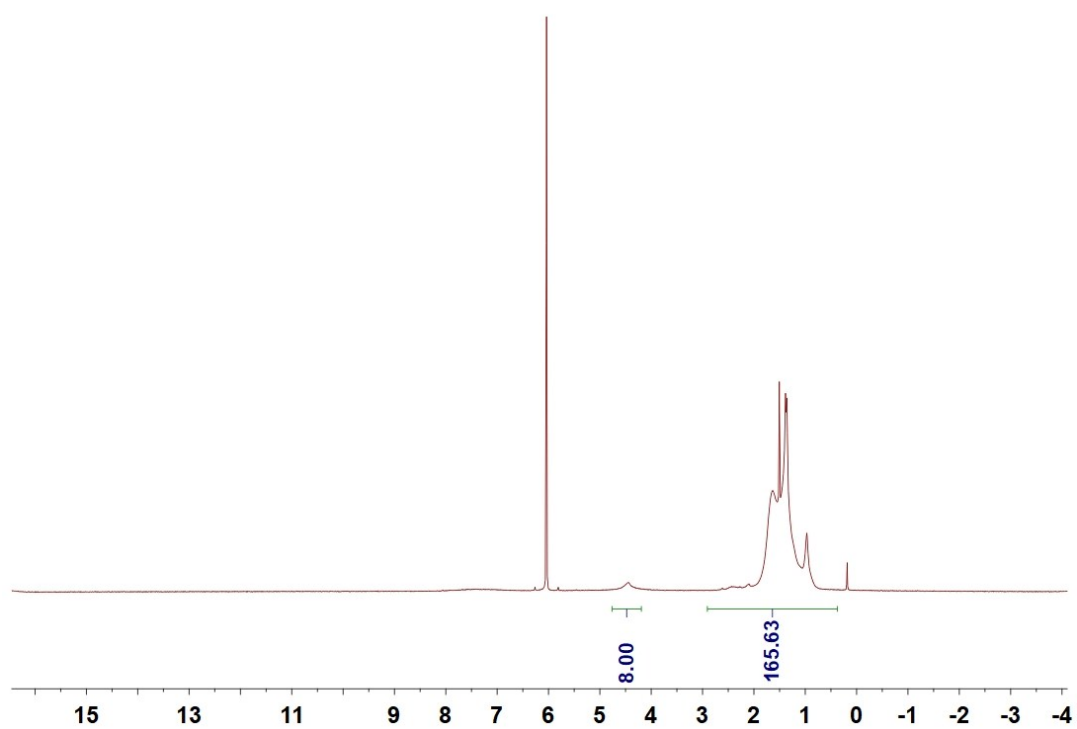


Figure S11. ¹H NMR spectrum of PBTI2(30DT)-FT.

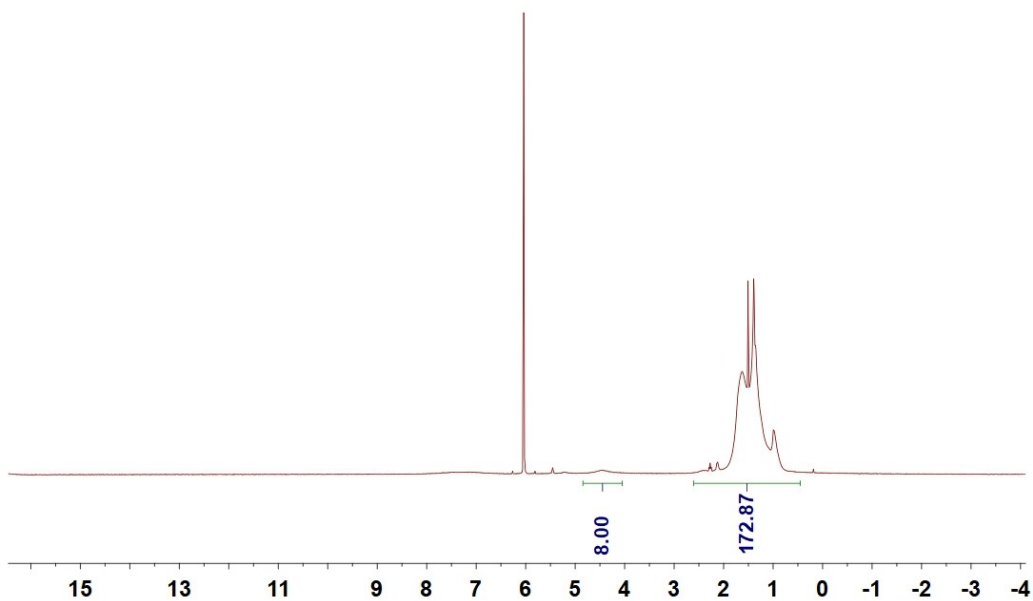


Figure S12. ^1H NMR spectrum of PBTI2(50DT)-FT.

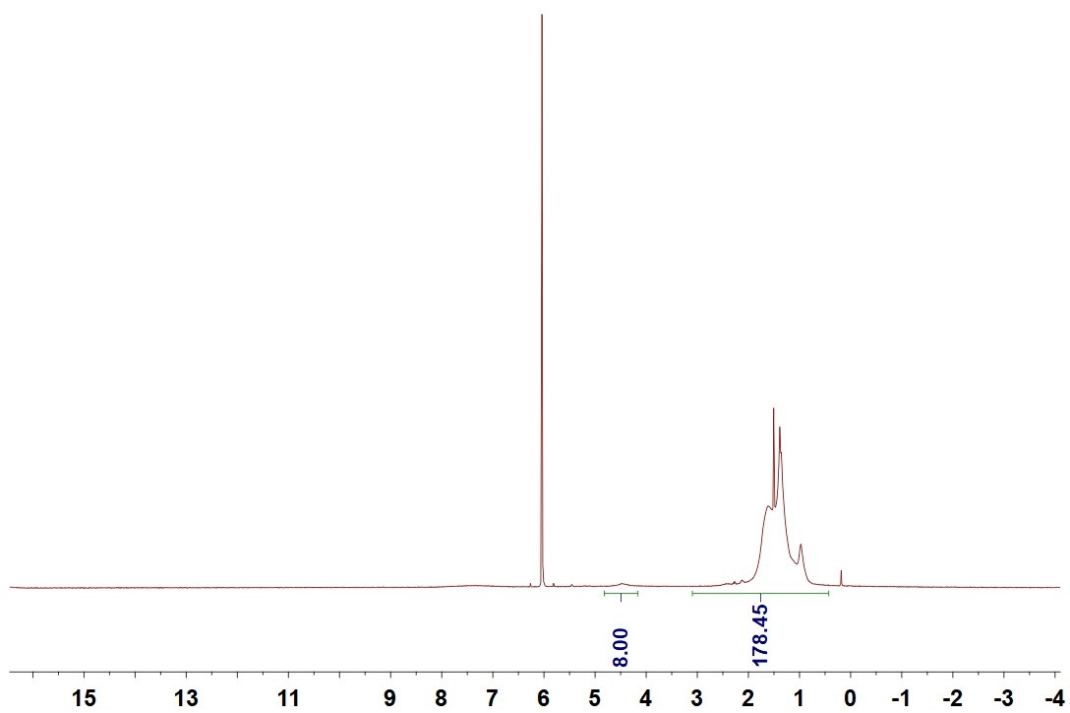


Figure S13. ^1H NMR spectrum of PBTI2(70DT)-FT.

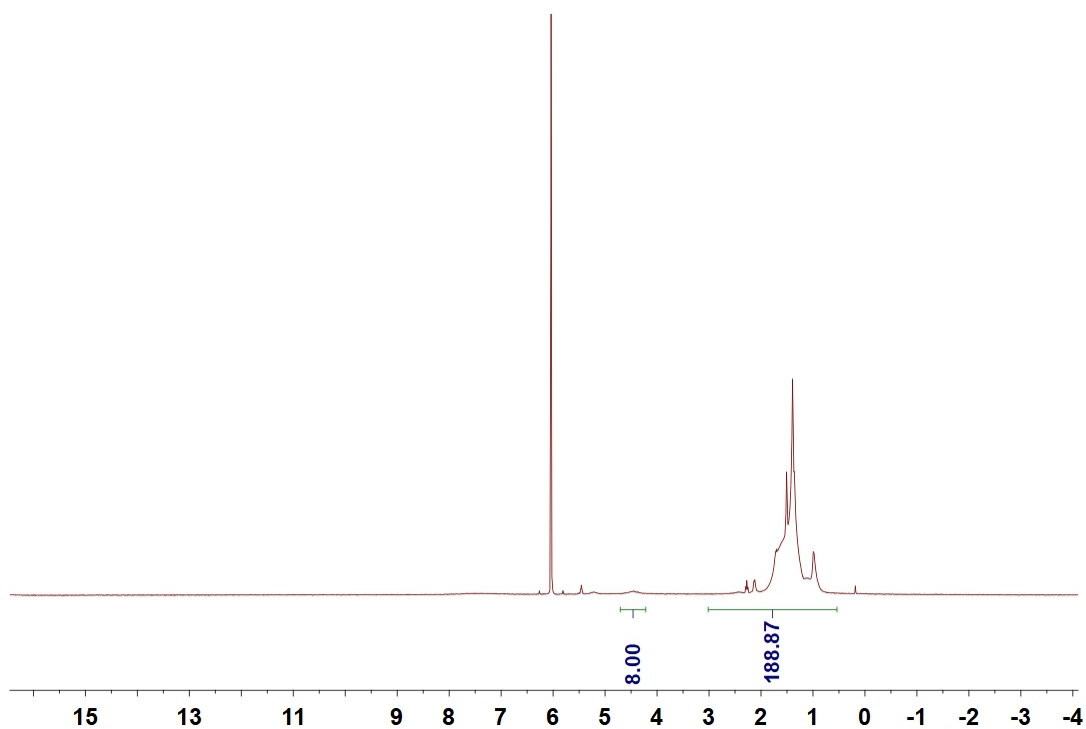


Figure S14. ¹H NMR spectrum of **PBTI2(100DT)-FT**.

Reference:

1. M. Saito, I. Osaka, Y. Suda, H. Yoshida and K. Takimiya, *Adv. Mater.*, 2016, **28**, 6921-6925.
2. Y. Wang, Z. Yan, H. Guo, M. A. Uddin, S. Ling, X. Zhou, H. Su, J. Dai, H. Y. Woo and X. Guo, *Angew. Chem. Int. Ed.*, 2017, **56**, 15304-15308.